PROCEEDINGS OF SCIENCE

Comparison of the data on proton-proton and proton-antiproton interactions at high energies on basis of the Low Constituents Number Model

V.A. Abramovsky*
Novgorod State University
Veliky Novgorod, Russia
E-mail: `Victor.Abramovsky@novsu.ru`

N.V. Abramovskaya
Novgorod State University
Veliky Novgorod, Russia
E-mail: `nvrad@mail.ru`

We argue that hadrons production is different in $p\bar{p}$ and pp interactions at high energies. There is process of hadrons production from three quark strings in $p\bar{p}$ which is absent in pp. This process grows as $(\ln\sqrt{s})^2$ and becomes significant when energy of collision increases. Inclusive cross sections of $p\bar{p}$ interaction exceed inclusive cross sections of pp. The UA1 data on $p\bar{p}$ transverse momentum distribution are about 1.2 – 1.3 times higher than the CMS, ATLAS and ALICE data on pp at energy $\sqrt{s} = 900$ GeV. Question regarding existence of the Pomranchuk theorem demands further investigation on evidence of difference of multiple processes in $p\bar{p}$ and pp interactions.

XXI International Baldin Seminar on High Energy Physics Problems,
September 10-15, 2012
JINR, Dubna, Russia

*Speaker.

PoS(Baldin ISHEPP XXI)070

1. Introduction

The Collaborations CMS [1], ATLAS [2] and ALICE [3] have published inclusive charged particle transverse momentum distributions in pp interaction at center-of-mass energy $\sqrt{s} = 900$ GeV[1]. The ATLAS and ALICE compared their measurements to inclusive cross sections of $p\bar{p}$ interaction obtained by the UA1 Collaboration [6] at the same energy $\sqrt{s} = 900$ GeV. The UA1 data overlaid with the ATLAS, ALICE and CMS data are shown in Fig.1. As an immediate consequence of Fig.1, the ratio of $p\bar{p}$ to pp inclusive cross sections at the same energy $\sqrt{s} = 900$ GeV

$$R = \left[\frac{1}{2\pi p_T}\frac{\mathrm{d}^2 n_{ch}^{p\bar{p}}}{\mathrm{d}\eta\,\mathrm{d}p_T}\right] \Bigg/ \left[\frac{1}{2\pi p_T}\frac{\mathrm{d}^2 n_{ch}^{pp}}{\mathrm{d}\eta\,\mathrm{d}p_T}\right] \tag{1.1}$$

is greater than unity, $R \simeq 1.2$ for the ATLAS and ALICE data and $R \simeq 1.3$ for the CMS data.

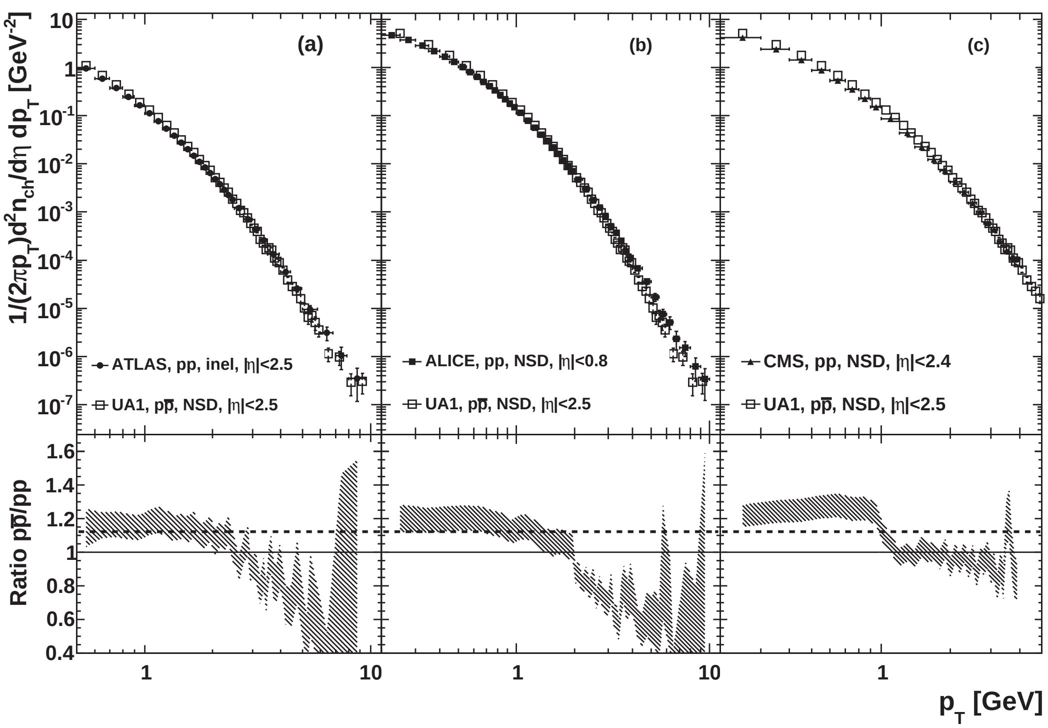

Figure 1: The ratios of invariant inclusive cross sections of the UA1 [6] to ATLAS [2] (a), ALICE [3] (b) and CMC [1] (c) at $\sqrt{s} = 900$ GeV. The shaded areas indicate the errors of the ratios. The dashed line shows the value of ratio $R = 1.12$, our prediction from the LCNM. The solid line at unity is shown for visibility.

[1] We define invariant inclusive cross section in standard form after pioneer papers [4, 5] $E\frac{\mathrm{d}^3\sigma}{\mathrm{d}p^3} = \frac{1}{2\pi p_T}\frac{\mathrm{d}^2\sigma}{\mathrm{d}y\,\mathrm{d}p_T} = \frac{1}{2\pi p_T}\frac{E}{p}\frac{\mathrm{d}^2\sigma}{\mathrm{d}\eta\,\mathrm{d}p_T}$. Here E, p – energy and momentum of observed particle, p_T – its transverse momentum, y – rapidity and η – pseudorapidity. Multiplicity density with respect to transverse momentum in unit of rapidity $\frac{\mathrm{d}^2 n_{ch}}{\mathrm{d}y\,\mathrm{d}p_T} = \frac{1}{\sigma}\frac{\mathrm{d}^2\sigma}{\mathrm{d}y\,\mathrm{d}p_T}$ or pseudorapidity $\frac{\mathrm{d}^2 n_{ch}}{\mathrm{d}\eta\,\mathrm{d}p_T} = \frac{1}{\sigma}\frac{\mathrm{d}^2\sigma}{\mathrm{d}\eta\,\mathrm{d}p_T}$. Value of σ can be picked either as $\sigma = \sigma_{inel}$ (inelastic) or as $\sigma = \sigma_{NSD}$ (non single diffractive) cross sections depending on various experimental methodologies. Notations of ATLAS and ALICE therefore can be written as $\frac{1}{N_{ev}}\frac{\mathrm{d}^2 N_{ch}}{\mathrm{d}\eta\,\mathrm{d}p_T} = \frac{\mathrm{d}^2 n_{ch}}{\mathrm{d}\eta\,\mathrm{d}p_T}$, notation of CMS can be written as $E\frac{\mathrm{d}^3 N_{ch}}{\mathrm{d}p^3} = \frac{1}{\sigma}E\frac{\mathrm{d}^3\sigma}{\mathrm{d}p^3}$.

The ATLAS and ALICE state that the difference is bound to systematic uncertainties of the UA1 experiment. The CMS did not compare their data on p_T distribution with the UA1 data and made no comments.

The Pomeranchuk theorem states that total, elastic and differential elastic cross sections of pp and $p\bar{p}$ interactions are equal at asymptotic high energies. It is commonly believed that characteristics of multiple production such as, for example, invariant inclusive cross section $E\mathrm{d}^3\sigma/\mathrm{d}p^3$ are also equal for pp and $p\bar{p}$ interactions at high energies. So it is expected that at high energies there must be equality $R = 1$ and experimentalists naturally try to explain the ratio $R > 1$ by the UA1 uncertainties.

The purpose of the present report is to argue that inclusive cross sections of $p\bar{p}$ interactions are higher than pp at the same energy. Thus experimental data of the CMS, ATLAS and ALICE do correspond to reality.

2. Inclusive cross sections of the CDF and CMS Collaborations

Our first argument is based on analysis of the CDF data on $p\bar{p}$ interactions at $\sqrt{s} = 1.96$ TeV [7] together with the CMS data on pp interactions at $\sqrt{s} = 2.36$ TeV [1]. We calculated the ratio of $E\mathrm{d}^3\sigma^{p\bar{p}}/\mathrm{d}p^3$ to $E\mathrm{d}^3\sigma^{pp}/\mathrm{d}p^3$ which is shown in Fig.2. The result is amazing – the ratio of inclusive cross sections equals unity with good accuracy. If we accept that $E\mathrm{d}^3\sigma^{p\bar{p}}/\mathrm{d}p^3 = E\mathrm{d}^3\sigma^{pp}/\mathrm{d}p^3$ at the same energy, these cross sections must be different as the energy increases by 400 GeV. That is, $E\mathrm{d}^3\sigma^{pp}/\mathrm{d}p^3$ at $\sqrt{s} = 2.36$ TeV must be higher than $E\mathrm{d}^3\sigma^{p\bar{p}}/\mathrm{d}p^3$ at $\sqrt{s} = 1.96$ TeV. Therefore the ratio given in the lower panel of Fig.2 must be systematically lower than unity.

Let us discuss some details of our analysis. Since there are no measurements of $p\bar{p}$ cross sections (total, inelastic or NSD) at $\sqrt{s} = 1.96$ TeV, we obtained the inclusive cross section $E\mathrm{d}^3\sigma^{pp}/\mathrm{d}p^3$ from the CMS data $\frac{1}{2\pi p_T}\frac{\mathrm{d}^2N_{ch}}{\mathrm{d}\eta\,\mathrm{d}p_T}$ [1] multiplied by σ_{NSD}. We used value $\sigma_{NSD} = 49.86$ mb which was estimated by the ALICE for $\sqrt{s} = 2.36$ TeV [8]. (Lower value $\sigma_{NSD} = 48.77$ mb which gives lower value of pp inclusive cross section was obtained in [9].) Therefore the experimental ratio given in Fig. 2 presumably confirms our assumption that $E\mathrm{d}^3\sigma^{p\bar{p}}/\mathrm{d}p^3 > E\mathrm{d}^3\sigma^{pp}/\mathrm{d}p^3$ at the same energy.

3. Subprocesses of multiple production in pp and $p\bar{p}$

In this section we will argue that it is possible to explain the difference in inclusive spectra of pp and $p\bar{p}$ interactions. Previously we have demonstrated the possibility of difference in multiplicity distributions in pp and $p\bar{p}$ scatterings [10]. It is almost impossible to prove this difference experimentally. But we can use this approach to analyze possible inequality in $E\mathrm{d}^3\sigma^{p\bar{p}}/\mathrm{d}p^3$ and $E\mathrm{d}^3\sigma^{pp}/\mathrm{d}p^3$. We are based on the Low Constituents Number Model (LCNM) [11, 12]. As it should be in any collision theory, the model contains three stages: preparation of initial state, interaction, and separation of reaction products. Schematic illustration of hadrons interaction and multiple production in this model is given by phenomenological diagrams in Fig.3.

A key feature of the model is assumption that there are only few scatters (constituents) in initial state of each colliding hadrons – these are valence quarks (antiquarks) and only one gluon.

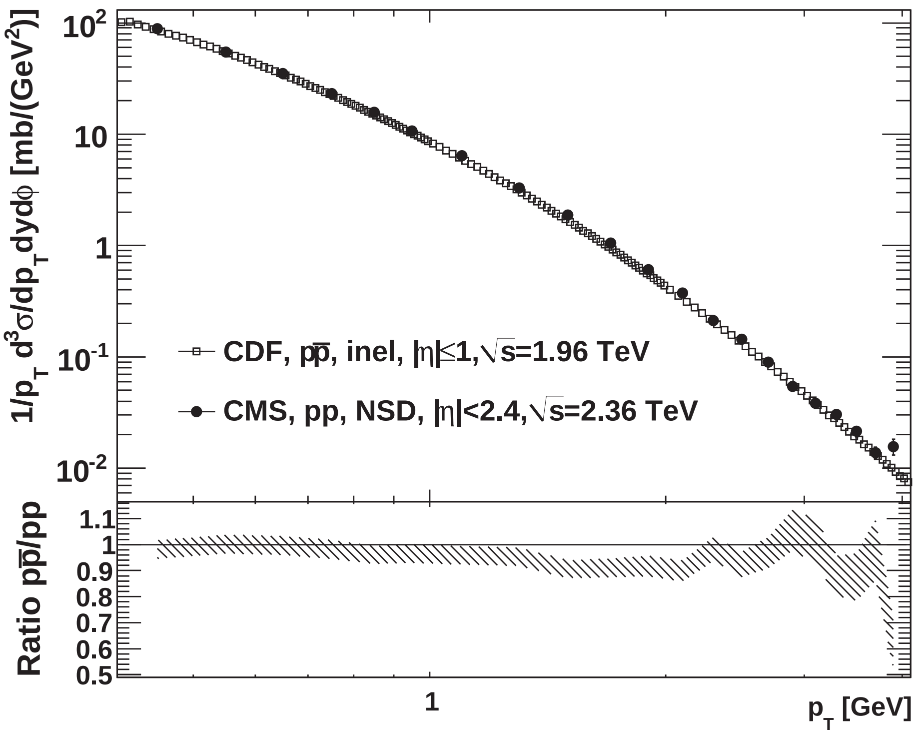

Figure 2: The ratio of invariant inclusive cross sections of CDF [7] at $\sqrt{s} = 1.96$ TeV to CMS [1] at $\sqrt{s} = 2.36$. The shaded area indicates the errors of the ratio. The solid line at unity is shown for visibility.

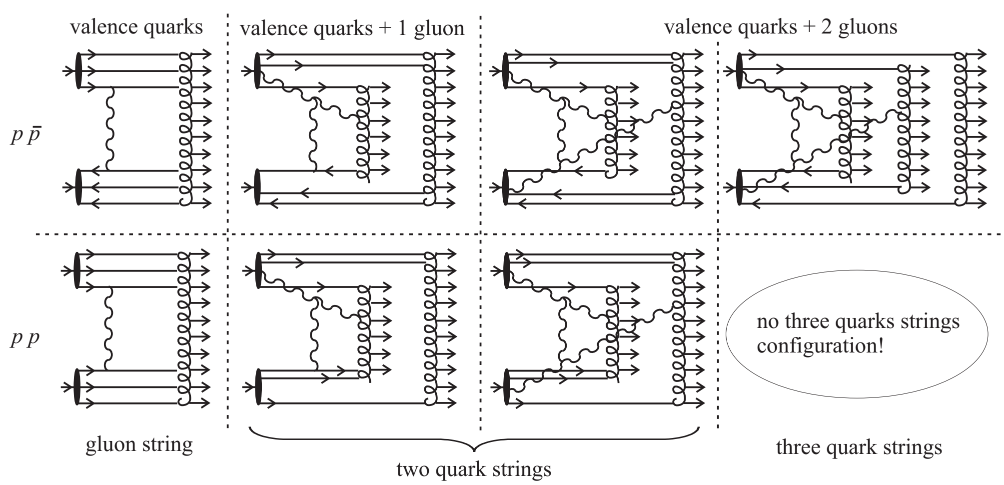

Figure 3: Three types of inelastic subprocesses in $p\bar{p}$ and pp scattering in the LCNM. Solid lines correspond to valence quarks and antiquarks, wavy lines are gluons. Color field string is shown as spiral. The initial state can be composed of either only valence quarks or valence quarks plus 1 or 2 gluons. The final state is different for pp and $p\bar{p}$ – there is no three quark strings configuration in pp interaction.

This gluon appears with low probability which grows slowly as energy increases[2]. Interaction

[2]This assumption allows to explain small value of the Pomeranchuk trajectory slope [11]. It also allows to describe

is carried out by gluon exchange which corresponds to Low–Nussinov two-gluon pomeron [13]. Due to gluon exchange colorless hadrons gain color charge. Separation of reaction products (colored hadrons) occurs after interaction. When the charges are separated by distance larger than the confinement radius, color electric field strings are produced. These strings break up to primary hadrons. Formation of color field string and its breakup into primary hadrons corresponds to the interaction in the final state.

It should be emphasized that because color objects are not emitted, the process of converting color charges to hadrons occurs with probability which equals to unity and does not affect interaction probability. Therefore values of total cross sections for both pp and $p\bar{p}$ are defined only by one gluon exchange in the second stage and so they are the same. Thus the Pomeranchuk theorem is fulfilled in the proposed LCNM approach.[3]

We distinguish the following inelastic processes of hadrons production (or they might be better defined as inelastic subprocesses in multiple hadron production) in pp and $p\bar{p}$ interactions.

Hadrons production from decay of gluon string. Gluon string is produced when objects carrying octet quantum numbers fly apart after interaction. In this case it is impossible to separate gluon from valence quarks. Wavelength of the gluon is such, that it overlaps with the valence quarks. This subprocess gives constant contribution to total cross sections. This subprocess is the same for both pp and $p\bar{p}$ interactions (Fig.3, first column).

Hadrons production from decay of two quark strings. Quark strings are produced between quark and antiquark and between diquark and antidiquark in $p\bar{p}$ interaction and between quark and diquark in pp interaction. Since gluon spectrum is $d\omega/\omega$ (ω – gluon energy), contribution from the component with one gluon in the initial state grows as $\ln\sqrt{s}$. This gluon is absorbed after the interaction by one of the quark strings, and it changes the string color charge – “recolor” the string. This contribution is the same for both pp and $p\bar{p}$ interactions (Fig.3, second column).

The contribution from two gluons in the initial state grows as $(\ln\sqrt{s})^2$. Both gluons are absorbed by quark strings “recoloring” them. In case of pp interaction the two gluons initial state can only give configuration with two quark strings in the final state (Fig.3, third column).

Hadrons production from decay of three quark strings. In case of $p\bar{p}$ interaction the two gluons initial state besides the configuration with two quark strings can lead to configuration with three quark strings (Fig.3, fourth column). The quark strings are produced between each quark and each antiquark. Since the contribution of this subprocesses grows as $(\ln\sqrt{s})^2$, it is quite essential at high energies[4].

We suppose that difference in inclusive cross sections in pp and $p\bar{p}$ interactions is governed by presence of three quark strings in $p\bar{p}$. This subprocess gives contribution in multiplicity distribution P_n in the region of high n (n - number of charged particles). In this region the value of P_n is about one order of magnitude smaller than in the maximum region and so it is hard to experimentally study it because of large uncertainties. Therefore the difference in P_n distributions in pp and $p\bar{p}$

value and growth with energy of pp, $p\bar{p}$, $\pi^{\pm}p$, $K^{\pm}p$ total cross sections [12].

[3]This argument is quite plausible, but it demands theoretical justification.

[4]Our approach is different from approach with exchange of decameron [14], which gives difference in multiplicity distributions and inclusive cross sections in pp and $p\bar{p}$ interactions. Contribution from decameron is low and constant with energy [14]. The AFS [15] and UA5 [16] Collaborations have not found this contribution at energy $\sqrt{s} = 53$ GeV. Moreover it will not be seen at higher energies.

interactions will be difficult to detect. One has to use another observable value, which is able to increase the difference between P_n distributions in pp and $p\bar{p}$ scatterings. We propose to use nP_n as the required observable value.

Let us define inclusive cross section of one charged particle production in an event with n charged particles – a topological inclusive cross section ("semi-inclusive" cross section of Koba, Nielsen and Olesen [17])

$$E\frac{\mathrm{d}^3\sigma_n}{\mathrm{d}p^3}, \quad \int \mathrm{d}p^3 \frac{\mathrm{d}^3\sigma_n}{\mathrm{d}p^3} = n\sigma_n, \tag{3.1}$$

where σ_n – topological cross section of n charged particles production. We consider here only non single diffractive events, so $\sum_n \sigma_n = \sigma_{NSD}$. We stress that (3.1) is normalized to $n\sigma_n$, where n – number of particles in an event.

In what follows we are based on the UA5 Collaboration data [18] on the inclusive cross sections in 9 multiplicity bins: $2 \leqslant n \leqslant 10$, $12 \leqslant n \leqslant 20$, $\ldots$, $n \geqslant 82$ at energy $\sqrt{s} = 900$ GeV. We define inclusive cross sections in bin (i)

$$\frac{\mathrm{d}^3\sigma^{(i)}}{\mathrm{d}p^3} = \sum_{n \text{ in bin } (i)} \frac{\mathrm{d}^3\sigma_n}{\mathrm{d}p^3} \tag{3.2}$$

which are normalized as follows

$$\int \mathrm{d}p^3 \frac{\mathrm{d}^3\sigma^{(i)}}{\mathrm{d}p^3} = \sigma_{NSD} \sum_{n \text{ in bin } (i)} nP_n = \sigma_{NSD}\,\bar{n}^{(i)}. \tag{3.3}$$

Here $P_n = \sigma_n/\sigma_{NSD}$ – probability of n charged particles production in a NSD event. Since we belive that inclusive cross sections of pp and $p\bar{p}$ are different we write down relation (3.3) separately for pp and $p\bar{p}$. It was shown in [19] that single diffractive cross sections σ_{SD} are the same for pp and $p\bar{p}$ interactions. Therefore $\sigma_{NSD} = \sigma_{tot} - \sigma_{el} - \sigma_{SD}$ are also the same.

From ratio of pp to $p\bar{p}$ in (3.3) we obtain the following relation

$$\int \mathrm{d}p^3 \frac{\mathrm{d}^3\sigma^{(i)}_{pp}}{\mathrm{d}p^3} = \frac{\bar{n}^{(i)}_{pp}}{\bar{n}^{(i)}_{p\bar{p}}} \int \mathrm{d}p^3 \frac{\mathrm{d}^3\sigma^{(i)}_{p\bar{p}}}{\mathrm{d}p^3}. \tag{3.4}$$

Value of $\bar{n}^{(i)}_{pp}/\bar{n}^{(i)}_{p\bar{p}}$ does not depend on momentum of observed particle p. Besides, bin limits can be chosen arbitrary. Therefore one of solutions of (3.4) (perhaps, the only solution) has the form

$$\frac{\mathrm{d}^3\sigma^{(i)}_{pp}}{\mathrm{d}^3p} = \frac{\bar{n}^{(i)}_{pp}}{\bar{n}^{(i)}_{p\bar{p}}} \frac{\mathrm{d}^3\sigma^{(i)}_{p\bar{p}}}{\mathrm{d}^3p}. \tag{3.5}$$

(If pp and $p\bar{p}$ interactions are the same, we obtain a trivial result.) The relation for the inclusive pseudorapidity cross sections in bin (i) is

$$\frac{\mathrm{d}\sigma^{(i)}_{pp}}{\mathrm{d}\eta} = \frac{\bar{n}^{(i)}_{pp}}{\bar{n}^{(i)}_{p\bar{p}}} \frac{\mathrm{d}\sigma^{(i)}_{p\bar{p}}}{\mathrm{d}\eta}. \tag{3.6}$$

We calculated the values of $\bar{n}^{(i)}_{p\bar{p}}$ from the UA5 data in each bin. The values of $\bar{n}^{(i)}_{pp}$ are calculated from multiplicity distribution P^{pp}_n, obtained in frame of LCNM [10]. Then we obtained inclusive pseudorapidity cross section for pp interaction at $\sqrt{s} = 900$ GeV.

$$\frac{\mathrm{d}\sigma_{pp}}{\mathrm{d}\eta} = \sum_i \frac{\mathrm{d}\sigma^{(i)}_{pp}}{\mathrm{d}\eta} = \sum_{i=1}^{9} \frac{\bar{n}^{(i)}_{pp}}{\bar{n}^{(i)}_{p\bar{p}}} \frac{\mathrm{d}\sigma^{(i)}_{p\bar{p}}}{\mathrm{d}\eta} \tag{3.7}$$

The values of the inclusive cross sections $\mathrm{d}\sigma_{p\bar{p}}/\mathrm{d}\eta$ and $\mathrm{d}\sigma_{pp}/\mathrm{d}\eta$ are shown in Fig.4 for whole multiplicity range (a) and for multiplicity from 62 to 70 (b). In this multiplicity bin the difference in the inclusive cross sections is very large because of high values of n.

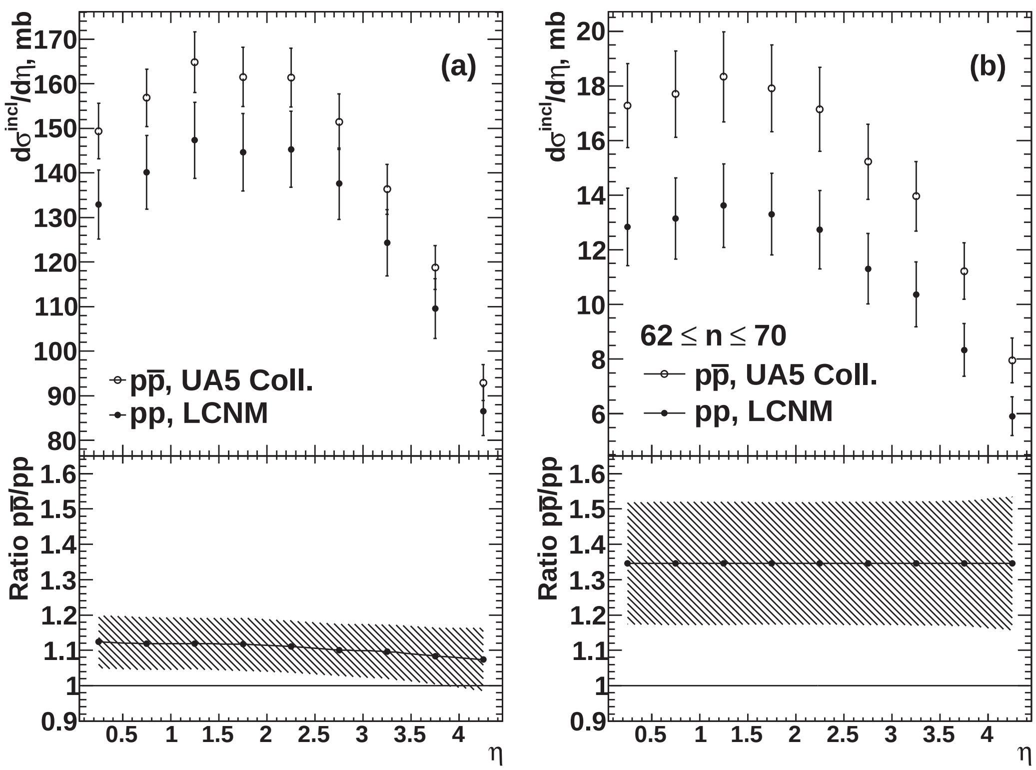

Figure 4: Inclusive cross sections at $\sqrt{s} = 900$ GeV. The points for $p\bar{p}$ were obtained from the UA5 data [18], the points for pp were obtained from the calculations in the LCNM. (a) Inclusive cross section for all charged particles. (b) Inclusive cross section for charged multiplicity bin $62 \leqslant n \leqslant 70$.

Factorization of inclusive cross sections results from the Abramovsky–Gribov–Kacheli (AGK cancellations) theorem [20]. Phenomenological factorization relations were proposed by Hagedorn [21] and Tsallis [22]. Therefore we can write down separate formulas for pp and $p\bar{p}$

$$\frac{1}{2\pi p_\mathrm{T}} \frac{\mathrm{d}^2\sigma_{pp}}{\mathrm{d}\eta\,\mathrm{d}p_\mathrm{T}} = f_{pp}(p_\mathrm{T}) \frac{\mathrm{d}\sigma_{pp}}{\mathrm{d}\eta}, \quad \frac{1}{2\pi p_\mathrm{T}} \frac{\mathrm{d}^2\sigma_{p\bar{p}}}{\mathrm{d}\eta\,\mathrm{d}p_\mathrm{T}} = f_{p\bar{p}}(p_\mathrm{T}) \frac{\mathrm{d}\sigma_{p\bar{p}}}{\mathrm{d}\eta}. \tag{3.8}$$

It is easy to obtain from the relations (3.4) – (3.8) that $f_{pp}(p_\mathrm{T}) \equiv f_{p\bar{p}}(p_\mathrm{T})$. One can obtain from (3.8) the following ratio

$$\left(\frac{1}{2\pi p_\mathrm{T}} \frac{\mathrm{d}^2\sigma_{p\bar{p}}}{\mathrm{d}\eta\,\mathrm{d}p_\mathrm{T}} \right) \Big/ \left(\frac{1}{2\pi p_\mathrm{T}} \frac{\mathrm{d}^2\sigma_{pp}}{\mathrm{d}\eta\,\mathrm{d}p_\mathrm{T}} \right) = \frac{\mathrm{d}\sigma_{p\bar{p}}}{\mathrm{d}\eta} \Big/ \frac{\mathrm{d}\sigma_{pp}}{\mathrm{d}\eta} = R. \tag{3.9}$$

It should be noted that the relations (3.8), (3.9) must be fulfilled in region of soft physics where the AGK theorem is valid. Therefore the relation (3.9) must be fulfilled for transverse momenta up to $p_T = 1.5 \div 2$ GeV. As it can be seen in Fig.4, the ratio of the inclusive cross sections is approximately equal to $R \simeq 1.12$. We can write down more strictly $R = 1.12 \pm 0.03$ [23]. On basis of relation (3.9) we can state that ratio of inclusive cross sections of $p\bar{p}$ to pp is equal to 1.12 ± 0.03. This value is depicted in Fig.1 by dashed line.

4. Discussion

We have shown that excess of $p\bar{p}$ inclusive cross section over pp inclusive cross section at the same energy is connected with hadrons production in three quarks string configuration in $p\bar{p}$, which is absent in pp interaction. We have predicted this difference in our paper [23] before the data of the CMS [1], ATLAS [2] and ALICE [3] were published. It should be noted that difference in pp and $p\bar{p}$ increases with rising collision energy in our approach[5]. We emphasize that we have a physical picture which was, probably, confirmed by results of the experiments UA1, CDF, CMS, ATLAS and ALICE.

We want to stress that discovery of an additional inelastic process in $p\bar{p}$ interaction is very important by itself. If existence of this process is experimentally proved, it will greatly change theoretical concepts of high energy physics. It is also important for Monte Carlo event generators which use data on pp and $p\bar{p}$ simultaneously in tuning of parameters, what may produce incorrect results.

5. Acknowledgements

We would like to thank A.V. Dmitriev and N.V. Prikhod'ko for useful discussions. This work was supportted by grant of RFBR 11-02-01395-a.

References

[1] V. Khachatryan et al. CMS Collaboration, JHEP 1002 (2010) 041, arXiv:1002.0621 [hep-ex].

[2] G. Aad et al. ATLAS Collaboration, Phys. Lett. B 688 (2010) 21, arXiv:1003.3124 [hep-ex].

[3] K. Aamodt et al. ALICE Collaboration, Phys. Lett. B 693 (2010) 53, arXiv:1007.0719 [hep-ex].

[4] A. H. Mueller, Phys. Rev. D 2 (1970) 2963.

[5] O. V. Kancheli, Pisma Zh. Eksp. Teor. Fiz. 11 (1970) 397.

[6] C. Albajar et al. UA1 Collaboration, Nucl. Phys. B 335 (1990) 261.

[7] T. Aaltonen et al. CDF Collaboration, Phys. Rev. D 79 (2009) 112005, arXiv:0904.1098 [hep-ex].

[8] M. G. Poghosyan for ALICE Collaboration, J. Phys. G 38 (2011) 124044, arXiv:1109.4510 [hep-ex].

[9] J. Bleibel, L. V. Bravina, A. B. Kaidalov, E. E. Zabrodin, arXiv:1011.2703 [hep-ph].

[10] V. A. Abramovsky, N. V. Radchenko, Phys. Part. Nucl. Lett. 6 (2009) 433.

[5] Three-sheet annihilation of Rossi–Veneziano [24] decreases as $s^{-1/2}$.

[11] V. A. Abramovsky, O. V. Kancheli, Pisma Zh. Eksp. Teor. Fiz. 31 (1980) 566;
V. A. Abramovsky, O. V. Kancheli, Pisma Zh. Eksp. Teor. Fiz. 32 (1980) 498.

[12] V. A. Abramovsky, N. V. Radchenko, Phys. Part. Nucl. Lett. 6 (2009) 368.

[13] F. E. Low, Phys. Rev. D 12 (1975) 163;
S. Nussinov, Phys. Rev. Lett. 34 (1975) 1286.

[14] B. Z. Kopeliovich, B. G. Zakharov, Phys. Lett. B 211 (1988) 221.

[15] T. Akesson et al. Axial Field Spectrometer Collaboration, Phys. Lett. B 108 (1982) 58.

[16] K. Alpgard et al. UA5 Collaboration, Phys. Lett. B 112 (1982) 183.

[17] Z. Koba, H. B. Nielsen, P. Olesen, Phys. Lett. B 38 (1972) 25.

[18] G. J. Alner et al. UA5 Collaboration, Z. Phys. C 33 (1986) 1.

[19] V. A. Abramovsky, arXiv:0911.4850 [hep-ph].

[20] V. A. Abramovsky, V. N. Gribov, O. V. Kancheli, Yad. Fiz. 18 (1973) 595.

[21] R. Hagedorn, Riv. Nuovo Cim. 6N10 (1984) 1.

[22] C. Tsallis, J. Stat. Phys. 52 (1988) 479.

[23] V. A. Abramovsky, N. V. Radchenko, arXiv:0912.1041 [hep-ph].

[24] G. C. Rossi, G. Veneziano, Nucl. Phys. B 123 (1977) 507.

[25] K. Aamodt et al. ALICE Collaboration, Eur. Phys. J. C 65 (2010) 111. arXiv:0911.5430 [hep-ex].

PoS(Baldin ISHEPP XXI)070